

# 1200 GHz High Spectral Resolution Receiver Front-end of Submillimeter Wave Instrument for Jupiter Icy Moon Explorer: Part I - RF Performance Optimization for Cryogenic Operation

J. Treuttel, L. Gatilova, S. Caroopen, A. Feret, G. Gay, T. Vacelet, J. Valentin, Y. Jin, A. Cavanna, K. Jacob, S. Mignoni, V. Lavignolle, J-M. Krieg, C. Goldstein, F. Courtade, C. Larigauderie, A. Ravanbakhsh, J-P. Garcia, A. Maestrini, P. Hartogh

**Abstract**—The Submillimeter Wave Instrument (SWI) is a spectrometer/radiometer instrument on board of Jupiter Icy Moons Explorer (JUICE) mission operating in two submillimeter heterodyne bands around 530  $\mu\text{m}$  (530 – 625 GHz) and 255  $\mu\text{m}$  (1080 – 1275 GHz). The paper presents the results of acceptance testing and performance optimization carried out on the flight and spare model of the 1200 GHz receiver front-end. The safe operation conditions at 120-150 K ambient temperature, such as maximum authorized input RF power, applied DC bias voltage are determined through the definition of the Schottky junctions dissipated power and current density ranges. A tuning procedure that optimizes the sensitivity of the front-end while keeping it within safe limits at 120-150K temperature operation is discussed. In part II, we present a detailed analysis of reliability and endurance testing.

**Index Terms**—Jupiter, Solar system, Space, Jupiter Icy Moon Explorer, Submillimeter Wave Instrument, Schottky diodes, receivers, Semi-conductor, Terahertz, Qualification.

## I. INTRODUCTION

The JUICE (JUPiter ICy moon Explorer) mission is the first large class mission (L1) within the ESA Cosmic Vision Program 2015–2025, to be launched in April 2023. JUICE will exploit in full the power of remote sensing synergy by combining moderate resolution imaging with very high-resolution point spectroscopy covering broad band spectral range from UV to sub-millimeter wavelengths.

This work was supported in part by Centre National d'Etude Spatial, in part by European Space Agency, (*Corresponding author: Jeanne Treuttel*).

J. Treuttel, L. Gatilova, A. Feret, G. Gay, T. Vacelet, J. Valentin, S. Mignoni, J-M. Krieg, are with Observatory of Paris-PSL (OBSPM-PSL), Laboratoire d'Etude du Rayonnement et de la Matière en Astrophysique (LERMA), 75014 Paris, France (e-mails: [jeanne.treuttel@obspm.fr](mailto:jeanne.treuttel@obspm.fr); [lina.gatilova@obspm.fr](mailto:lina.gatilova@obspm.fr); [alexandre.feret@obspm.fr](mailto:alexandre.feret@obspm.fr); [gregory.gay@obspm.fr](mailto:gregory.gay@obspm.fr); [thibaut.vacelet@obspm.fr](mailto:thibaut.vacelet@obspm.fr); [jerome.valentin@obspm.fr](mailto:jerome.valentin@obspm.fr); [sabrina.mignoni@obspm.fr](mailto:sabrina.mignoni@obspm.fr); [jean-michel.krieg@obspm.fr](mailto:jean-michel.krieg@obspm.fr)).

Y. Jin and A. Cavanna are with Center for Nanoscience and Nanotechnology (C2N), 10 Boulevard Thomas Gobert, 91120 Palaiseau, France (e-mails: [yong.jin@c2n.upsaclay.fr](mailto:yong.jin@c2n.upsaclay.fr); [antonella.cavanna@c2n.upsaclay.fr](mailto:antonella.cavanna@c2n.upsaclay.fr)).

K. Jacob, A. Ravanbakhsh, J-P. Garcia, P. Hartogh are with Max Planck Institute for Solar System Research (MPS), Göttingen, Germany (e-mails: [jacob@mps.mpg.de](mailto:jacob@mps.mpg.de); [ravanbakhsh@mps.mpg.de](mailto:ravanbakhsh@mps.mpg.de); [garciajp@mps.mpg.de](mailto:garciajp@mps.mpg.de); [hartogh@mps.mpg.de](mailto:hartogh@mps.mpg.de)).

For illustration, Fig. 1 compares the JUICE spectro-imaging capabilities with those of the Galileo mission.

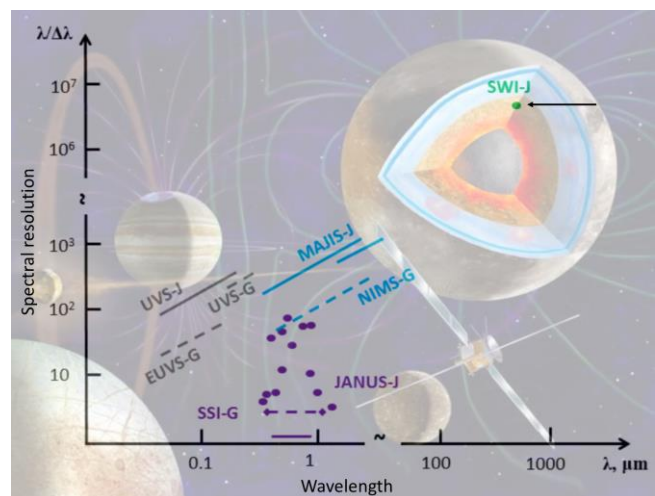


Fig. 1. Spectral resolving power vs. spectral range for the JUICE (solid lines and dots, labelled by “J” in the figure) and Galileo (dashed lines) spectro-imaging instruments (denoted by “G” in the figure labels) modified from [2].

In particular, the Submillimeter Wave Instrument (SWI) is a heterodyne spectrometer measuring spectra and continuum emissions in two bands between 530 – 625 and 1080 – 1275 GHz, Fig. 2(a). SWI’s spectrally tunable two independent front-ends channels serve to detect variation in THz radiation

C. Goldstein, F. Courtade, C. Larigauderie are with Centre National d’Etudes Spatiales (CNES), 18 avenue Edouard Belin, F-31401 Toulouse cedex 9, France (e-mails: [christophe.goldstein@cnes.fr](mailto:christophe.goldstein@cnes.fr); [frederic.courtade@cnes.fr](mailto:frederic.courtade@cnes.fr); [carole.larigauderie@cnes.fr](mailto:carole.larigauderie@cnes.fr)).

S. Caroopen was with Observatory of Paris-PSL, Laboratoire d’Etude du Rayonnement et de la Matière en Astrophysique (LERMA), 75014 Paris, France. He is now with AB Millimetre 52 rue Lhomond 75005 Paris, France. (e-mail: [abmillimetre@wanadoo.fr](mailto:abmillimetre@wanadoo.fr)).

V. Lavignolle is with EO IPSO, 138 chemin de baiza, 31660 Bessières, France (e-mail: [lavignolles@aol.com](mailto:lavignolles@aol.com)).

A. Maestrini was with Observatory of Paris-PSL, Laboratoire d’Etude du Rayonnement et de la Matière en Astrophysique (LERMA). He is now with Jet Propulsion Laboratory, California Institute of Technology, 4800 Oak Grove Drive, Pasadena, CA 91109, USA (e-mail: [alain.e.maestrini@jpl.nasa.gov](mailto:alain.e.maestrini@jpl.nasa.gov)). Color versions of one or more of the figures in this article are available online at <http://ieeexplore.ieee.org>

related to the physical temperature of optical blackbodies, at a magnitude below 0.1 Kelvin with 100 kHz spectral resolution, i.e up to  $10^7$  over 15% relative detection bandwidth [1], Fig. 2(c).

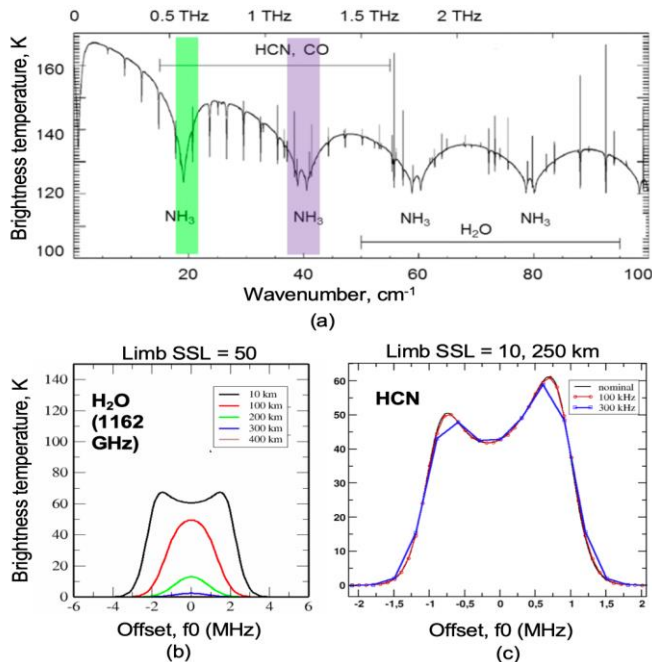


Fig. 2. (a) Synthetic microwave spectrum of Jupiter atmosphere modified from [2], 600 GHz (green) and 1200 GHz (violet) channels. High spectral resolution examples versus spectral resolution: (b) simulations of  $\text{H}_2\text{O}$  in Ganymede atmosphere at 1162 GHz (Limb spectra for different altitudes) [2] and (c) HCN line for different spectral resolution.

Therefore, SWI will enable access to the submillimeter portion of the spectrum with spectral resolution higher than ever achieved by any orbiting spacecraft around Jupiter [2], offering new capabilities in sounding of the spectral lines of the gases present in the upper atmosphere of the giant planet to determine composition, temperature structure and dynamics in its middle atmosphere. A feature of SWI includes simultaneous observation of several  $\text{H}_2\text{O}$  lines using the two channels. SWI merges heritage of a number of space borne microwave heterodyne spectrometers such as the Millimeter Wave Atmospheric Sounder (MAS) [3], [4], Odin [5], the Microwave Instrument for the Rosetta Orbiter (MIRO) [6] and the Heterodyne Instrument for the Far Infrared (HIFI) [7]. In our case, the mission duration is up to 9 years cruising to Jupiter and 3 years of operations. For the planned launch window in April 2023 the cruise phase involves one Venus and three Earth fly-bys. The science operation includes 2.7 years of Jupiter phase, 27 satellite flybys and 284 days of Ganymede orbit. Science observation scenarios have been defined for a various set of observation modes, which duration is typically of one hour each. The thermal environment is defined as five thermal

<sup>1</sup> LERMA contribution also includes the 300 GHz single chip frequency doubler as the last stage of the local oscillator (LO) of the 600 GHz channel but also other subsystems such as the regulator bias box (RBB) to supply regulated DC bias voltage to both the 1200 GHz mixer and its first stage LNA, the two

cases covering cruise phase and mode of operation of the instrument, in particular the science cases at Jupiter and its moons.

The high frequency part of the SWI instrument front-end feature GaAs-based Schottky-diode microwave monolithically integrated circuit (MMIC) devices especially designed and fabricated for the JUICE mission [8], [9], [10]. The 1200 GHz channel part procured by OBSPM-PSL consists of an assembled chain including a 300 GHz power-combined frequency doubler, a 600 GHz frequency doubler, and a 1200 GHz sub-harmonic mixer<sup>1</sup>. These components are the core devices of the receivers where the frequency conversion occurs. Interplanetary space missions imply particularly severe and specific constraints on devices reliability. The work presented here is the first part of the assessment and acceptance methodology developed to keep best performance levels, within safe limits, so that environmental and operational precautions can be appropriately placed to mitigate risks. In Section II, we describe the SWI radiometer front-end system and in Section III we discuss its key system design aspects in order to reach best noise temperature performances. The condition for safe DC tuning is the primary focus of the paper and is detailed in Section IV. The discussion encompasses the front-end element pre-calibration, before the full instrument commissioning campaign<sup>2</sup>. First, we focus on the definition of the Schottky junction's typical dissipated power and current density ranges as well as their monitoring during the Assembly, Integration and Test/Verification program (AIT/AIV) of the front-end only at 300 K room temperature. Then we describe additional cryogenic testing of the junctions, which parameters are injected in the modelling of the 1200 GHz front-end at the nominal 120-150 K temperature of operation [1]. Finally, we assess the safe tuning procedure developed in order to keep the instrument within safe limits between 120-150 K ambient temperature, and we define the typical and maximal thermal dissipation values allowed per anode area. In part II, we put in perspective reliability during operation, endurance testing and determine allowed tuning deviations.

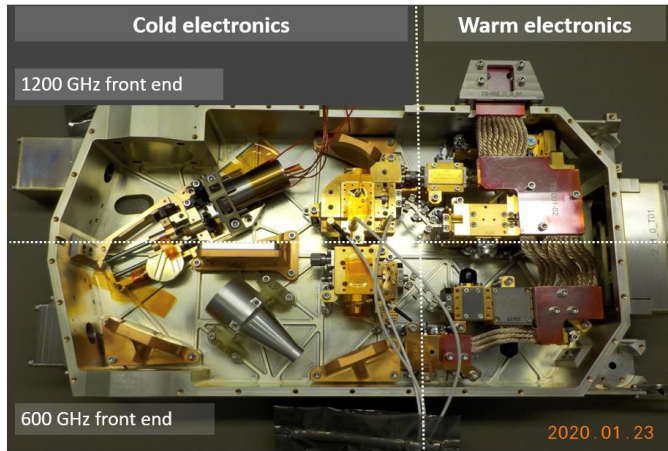
## II. RECEIVER UNITS (RU) AND OBSPM-PSL CONTRIBUTION

Figs. 3(a) and (b) show the SWI radiometer front-end Receiver Units (RU). The radiation/signal is collected by a diffraction limited elliptical reflector with projected 29 cm aperture and collimated via the mirror M2 into the Receiver Unit (RU). After entering the RU box, the beam encounters a planar mirror M3 and an elliptical mirror M4. A free-standing wire grid (WG) splits the beam into two orthogonal linear polarizations [11]. The reflected polarization component parallel to the wires is coupled via the elliptical mirror M5R to the feed-horn of the 600-GHz double sideband (DSB) Schottky-mixer and its integrated IF low noise amplifier

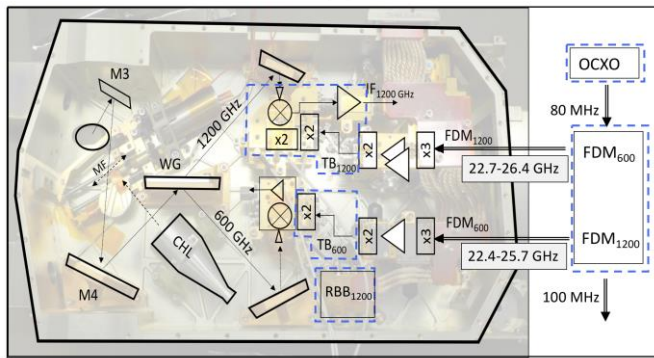
GHz thermal break titanium waveguide (interface from hot to cold electronics), the technical assessment of the dual K band synthesizer (designed and procured by Syrlinks), the 80 MHz  $10^{-8}$  Stability class ultra stable oscillator (procured by Rakon), the IF LNA (procured by Miteq) and the 1200 GHz horn (procured by RPG)[12].

<sup>2</sup> See further publications on SWI in "Space Science Review Paper".

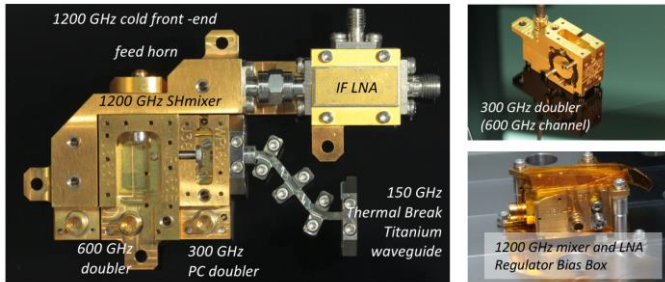
developed and fabricated by Chalmers [10]. The transmitted polarization component that is perpendicular to the wires is reflected from the elliptical mirror M5T to the feed-horn of the 1200-GHz DSB Schottky-mixer receiver.



(a)



(b)



(c)

Fig. 3. SWI Receiver Unit front-end. (a) Fully assembled Receiver Unit (courtesy MPS) with (b) simplified schematic (French contribution in dashed lines); OBSPM-PSL main contribution includes the cold electronics front-end (c): the 1200 GHz mixer plus cryo-LNA ensemble, DC bias regulator, LO last stage doubler at 300 GHz and 600 GHz, and the thermal titanium waveguide break interfacing with the 150 GHz source.

For the 1200 GHz channel, the signal enters a 1200 GHz spline horn [12] and is led to the sub harmonically pumped mixer (SHM) and down converted to an instantaneous 9 GHz frequency IF bandwidth double side band. The high purity and stability [13] local oscillator (LO) signal consists of a K-band synthesizer<sup>3</sup>, using a 80 MHz reference signal generated by a  $10^{-8}$  stability class space ultra stable oscillator (USO)<sup>4</sup>,

followed by E-band triplers, power amplifiers<sup>5</sup> and cascaded frequency doublers.

The 300 GHz [14] and 600 GHz [15] frequency doublers multiply by four the frequency of the input signal at 150 GHz interfaced with a thermal break waveguide made out of titanium. Requirements of the dual K band synthesizer have been specified for heterodyne detection at 600 GHz and at 1200 GHz, with a phase error at X band to be below  $0,22^\circ$  rms [16]. The down-converted signal at intermediate frequency band (IF signal) at 3.5-8.5 GHz<sup>6</sup> is amplified using a Low Noise Amplifier (LNA)<sup>7</sup> and fed to a high-resolution Chirp Transform Spectrometers and a broadband Autocorrelation Spectrometers.

OBSPM-PSL contribution encompasses the cold electronic front-end (1200 GHz mixer, 600 GHz and 300 GHz frequency doublers, LNA, and Regulator Bias Box (RBB)) illustrated in Fig. 3(b) and (c) as well as the K-band synthesizer or frequency distribution module as part of the electronic unit.

The acceptance of the FM and FSM models followed a methodology in accordance with planning constraints. The sequence started with separated mounting of the MMIC chips in their wave-guide blocks, followed by a series of screening tests (thermal cycling, burn-in, High Temperature Reverse Bias (HTRB)). Then the blocks showing best performance were selected and assembled in one flight (FM) and one spare (FSM) chains. Other blocks were assembled in qualification chains (QM) to demonstrate that hardware fulfil all specified requirements under simulated conditions more severe than those expected during the mission. DC bias look-up tables values obtained with the demonstrator model (DM) [15] at 300 K room temperature have been used as initial state to secure a traceability of the performances across all delivered models (Engineering Model, QM, FM/FSM). The screening and acceptance include RF heterodyne measurement for health control ending with a performance and pre-calibration campaign at 300 K and 120-150 K ambient temperatures.

### III. 1200 GHz FLIGHT MODEL CHANNEL PERFORMANCES DURING AIT/AIV PROGRAM

The minimum detectable temperature variation is  $\Delta T = T_{\text{sys}} / \sqrt{(B \cdot \tau)}$ , where  $\tau$  is the integration time and  $T_{\text{sys}}$  the system noise temperature. The specification of SWI 1200 GHz channel is a DSB noise temperature not larger than 4000 K with an optimum goal of 3000 K at 120-150 K over the full 1080-1275 GHz frequency bandwidth. The system performances have met the expectations with additional 1000K margin (Table I). This achievement offers SWI relaxed operating condition such as a factor square reduction in the integration time.

$T_{\text{sys}}$  is firstly dominated by the mixer noise, then by the noise of the IF LNA (because of the mixer conversion losses) as given by the Friis' noise factor cascaded formula. The 1200 GHz mixer features two DC series-connected sub-micronic Schottky diodes (with anode area of  $0,16 \mu\text{m}^2$ ) on a  $2 \mu\text{m}$  thick

<sup>3</sup> Procured by Syrlinks

<sup>4</sup> Procured by Rakon

<sup>5</sup> Procured by Radiometer Physics

<sup>6</sup> Nominal value of mixer IF output impedance matching.

<sup>7</sup> The LNA noise factor value is 0.9 to 1.3 dB over 3.5-8.5 GHz. LNA MITEQ SAFS3-03500850-10-CR-FM

substrate, optimized for state-of-the-art low noise parasitics at Terahertz frequency [17], [18] and 300 K room temperature. As illustrated in Fig. 4, the MMIC features a sub-harmonic balanced configuration that cancels out very efficiently the amplitude modulation noise (AM) [19]. In addition, because the noise contribution of a local oscillator drops off rapidly away from the carrier, the LO noise in a sub-harmonic (and balanced) mixer is much lower than for a fundamental balanced mixer [20]. An important specificity of the diode cell is that it integrates an on-chip capacitance, providing a local separation of the DC (Fig. 4(b)) and IF path (Fig. 4(c)). In this way, the varistor mode of the two Schottky diodes is secured by DC forward biasing, while offering the possibility to finely adjust the local oscillator power to a minimum at anode level for best receiver noise performance.

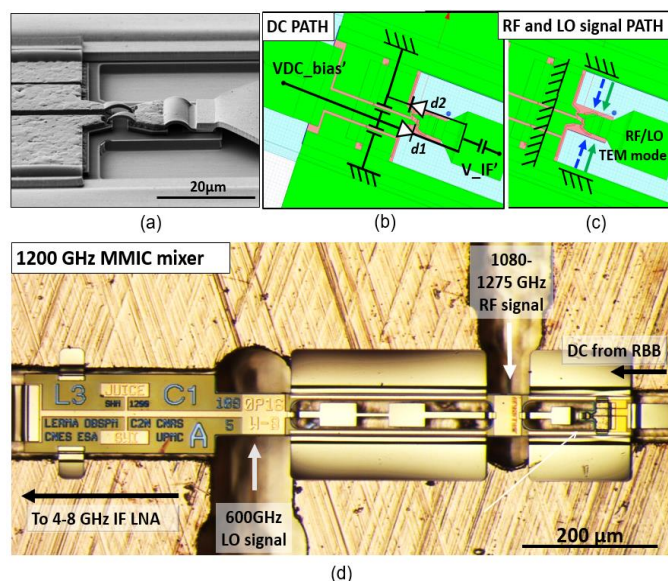


Fig. 4. SWI 1200 GHz MMIC mixer circuit with sub-micronic anti-parallel Schottky diodes. (a) Scanning electron microscope picture of the fabricated diode cell and its DC near vicinity on-chip capacitance, (b) DC and IF path at diodes vicinity, (c) RF and LO signal transmission modes, (d) chip mounted in its gold-plated mechanical block (micro-meter alignment accuracy from top to bottom).

Fig. 4(d) shows the fabricated 1200 GHz mixer after its release and mounting in the waveguide block. This block features micrometer alignment accuracy, and is made out of gold coated aluminum<sup>8</sup>. In addition, the metal waveguide block includes an AC filtering circuit after the DC ports, allowing to filter potential spurious at high frequency [21] thus adding high rejection in the IF band. This AC filtering circuits also provides redundant protection to potential electrostatic discharge events (ESD) during DC supplies switch ON and OFF transient steps. The 1200 GHz mixer bias voltage is supplied by the DC regulator bias box, and a real ground is applied when the output is not activated adding an ESD protection. The drawback is that the mixer diodes DC rectified current cannot be accessed therefore monitored during operation. The 300 GHz and 600 GHz frequency doublers (Fig. 5) also feature micronic anodes (of  $15,8 \mu\text{m}^2$  and  $3 \mu\text{m}^2$ , respectively) on MMIC chips,

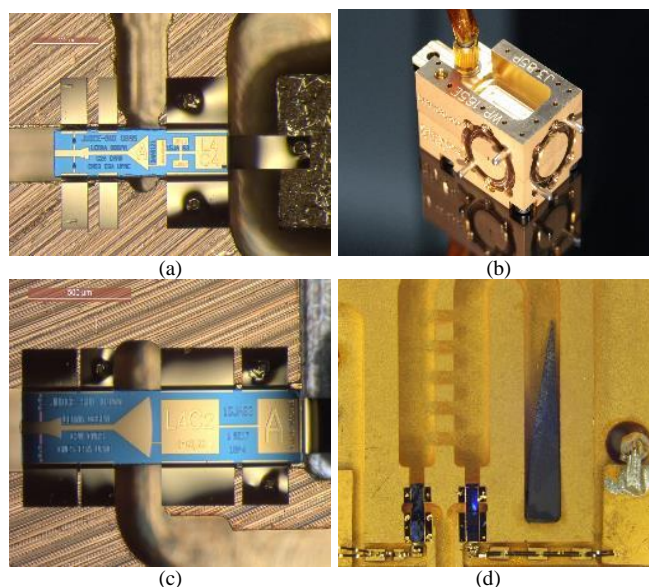


Fig. 5. SWI circuits. (a) 600 GHz single chip MMIC doubler and (b) its final mounted mechanical block with flange and DC interface connector, (c) 300 GHz MMIC doubler and (d) 300 GHz power combined dual chip doubler with hybrid and load.

operating this time in varactor mode with reverse DC bias voltage operation [22]. Contrarily to the mixer, the frequency doubler AC protecting circuit allows the monitoring of the rectified current during operation while they are AC-protected on their DC port.

During RF measurement, each element of the LO power of the 1200 GHz mixer as well as the mixer itself, are DC tuned to given frequency-dependent values in order to finely adjust impedance matching and limit interface mismatch ripples. This look-up table constitutes the initial values for calibration and commissioning phases of the instrument at MPS. Table I gives the measurement performances of the FM and FSM chains and some of the identified molecular lines<sup>9</sup>. The molecular line frequencies are based on [23] for most neutral compounds and [24] for most ions species.

Although FSM has overall better performance than the FM, FSM won't be installed if no significant failure of the FM occurs during the instrument integration process into the JUICE platform.

As it was already mentioned, special attention should be given to the device reliability that involves a definition of failure, time, and statistic. Submicronic GaAs/metal contact anodes have already been reported to degrade or fail with excessive amounts of either forward or reverse currents. As discussed in [25], measured I/V characteristics show that in small diodes the current deviates considerably from the ideal thermionic model behavior with decreasing diode diameter, caused either by edge effects and/or interface effects at the metal semiconductor junction. In addition, the diode finger can act as a fuse, making this parameter process and design related. Failure mechanisms have been studied and reported separately, associated with electrostatic discharge [26], [27], [28], Thermal

<sup>8</sup>The process is developed in collaboration with Société Audioise de Production and KERDY, France.

<sup>9</sup> The "tuning label" contains the name of the main observable molecule (e.g. H<sub>2</sub>O), as well as the approximate frequency in GHz (e.g. 1097), and the position of the line either in the lower ("L") or in the upper ("U") sideband.

cycling [14], temperature only induced failures (no DC nor RF excitation) [29] or temperature increase induced failures (equivalent to RF excitation) [30]. In part II, we will discuss the methodology to test the sequential peak and average degradation of the flight wafer representative to the all thermal or electrical risks. In the present paper, we define the limits of the pass criteria with the herein condition of safe RF optimization.

TABLE I

PERFORMANCES OF THE DELIVERED 1200 GHz CHANNEL OF THE SWI FLIGHT MODEL AND ASSOCIATED MOLECULAR LINES.

$F_{\text{Synthetizer}}$ (MHz)	$F_{\text{LO}}$ (GHz)	Molecular line	$T_{\text{REC DSB}}$	
			FM1	FS
22736.2500	1091.34	T-H2O-1097U	3040 K	2366 K
24520.8333	1177.00	Center frequency	2525 K	2205 K
24573.7500	1179.54	T-CS-1173L	2540 K	2259 K
25706.2500	1233.90	T-HCN-1239U	2503 K	2035 K
26043.7500	1250.10	T-CH4-1256U	2354 K	2122 K
26521.8750	1273.05	CO-1267L	2420 K	2318 K

#### IV. CONDITIONS OF SAFE RF OPTIMIZATION

During RF operation or RF performance tuning, the DC parameters, such as DC bias voltages (look-up table) and associated rectified currents should be limited to acceptable values, for each block of the 1200 GHz front-end individually (300 GHz, 600 GHz doublers and 1200 GHz mixer). Indeed, to guarantee that the diode will not be damaged during operation, the DC bias voltage must not exceed a certain range in order to avoid excessive currents in the positive or reverse directions and prevent any aging or damaging of the junction [30]. On one hand, constant reverse currents of few  $\mu\text{A}$  can degrade the diode even before the avalanche breakdown happens [22], because of the excess in voltage swing that might tackle reverse current and therefore should be limited [31]. On the other hand, the forward (and positive) current level reaches typically a few mA and hundreds of  $\mu\text{A}$  respectively for the multiplier and mixer, flows through the bias lines, and is absorbed by the load provided at the DC supply interface and also should be monitored and limited. Unfortunately, the peaks of the voltage swing is too fast and cannot be measured directly; only measurements of the average voltage and current are possible at these frequencies. In our case, voltage swing was verified through simulation and confirmed during RF endurance testing. For this reason, our power dissipation budget covers the typical and worst case of thermal dissipation (forward current) while it fulfills reverse voltage swing limitations tested with DC HTRB and RF endurance. To finely control the increase of multiplier efficiency at 120-150K temperature we implement RF optimization DC tuning to constrain to minimal compliant ranges. This tuning uses safe procedures and is confirmed by modelling in the following paragraphs and endurance testing in part II.

##### A. Power dissipation budget equations

Each of the multiplier and mixer diodes can sustain a certain amount of incoming and dissipated power expressed per junction area (in  $\text{mW}/\mu\text{m}^2$ ), related to a given forward DC current density during operation. The maximum of this forward DC current is limited by the diode's ability to dissipate heat

[32], and increases with doping density [30] and over time [29], [31]. The multipliers and mixer under analysis feature nonlinear balanced structures optimized for signal detection or generation, efficiency of which rely on first, second and/or idler harmonic matching [33]. At first order, the power dissipation budget can be identified at DC, first and second harmonics. This equilibrium state differs for the 300 GHz, 600 GHz doublers, and the 1200 GHz mixer, respectively. For this analysis, we consider a worst case, i.e. when all dissipated power dwell in a thermal dissipation only, located at the anode. The frequency doublers convert the input signal to an output power at a doubled frequency with a budget equilibrium noted as:

$$P_{\text{dissipated}} = P_{\text{Input } h1} - P_{\text{Output } h2} + P_{\text{DC varactor}} \quad (1a)$$

$P_{\text{dissipated}}$  is the total dissipated power in mW,  $P_{\text{Input } h1}$  and  $P_{\text{Output } h2}$  are respectively the doubler input and output signals at harmonics 1 and 2 ( $P_{\text{Input } h1} > P_{\text{Output } h2}$ ). with  $P_{\text{DC varactor}} = V_{\text{DC-bias Doubler}} \times I_{\text{DC Doubler}}$ ,  $V_{\text{DC-bias Doubler}}$  being the applied DC voltage tuning and  $I_{\text{DC Doubler}}$  the junction DC rectified current, flowing from DC anode to DC load. Both  $P_{\text{Input } h1}$  and  $P_{\text{Output } h2}$  contain transmission and reflection coefficients. Most of the time, the dissipated power is strictly the remaining portion of the non-converted power at harmonic 2, therefore decreases linearly with the increase of efficiency of the multiplier. Indeed, for the perfect frequency multiplier, the dissipated power at equilibrium reaches a maximum when pure varactor mode is excited at  $V_{\text{DC bias Doubler}} < 0$  and  $I_{\text{DC bias Doubler}} \rightarrow 0$ . However, the exact power dissipation budget of the real multiplier at full scale includes all matched-unmatched loaded harmonics and intermodulation products [32] such as:

$$P_{\text{dissipated}} = \sum [P_{\text{Input } hn} - P_{\text{Output } h(n+1)}] + P_{\text{DC varactor}} \quad (1b)$$

with  $hn$  being the  $n$ th harmonic of the signal passing through the Schottky anodes. In addition, both varactor and varistor mode co-exists, and most of the time  $I_{\text{bias Doubler}}$  remains positive, i.e. some part of the power is converted to a positive DC power.

In the mixer case, the energy budget is at first order related to the contribution of the mixing product  $f_{\text{IF}} = f_{\text{RF}} \pm f_{\text{LO}}$ . The mixer is DC biased with a positive voltage and a positive current appears due to RF rectification (nominal varistor operation) and the dissipated power is expressed as:

$$P_{\text{dissipated}} = P_{\text{RF input}} + P_{\text{LO input}} - P_{\text{IF Mixer}} - P_{\text{DC varistor}} \quad (2a)$$

with,  $P_{\text{DC varistor}} = V_{\text{DC bias Mixer}} \times I_{\text{DC Mixer}}$ ,  $V_{\text{DC bias Mixer}} > 0$  and  $I_{\text{DC}}$  is the junction DC rectified current, which flows from DC load to anode. The DC rectified current is typically on the order of several 100  $\mu\text{A}$ . The power of the RF signal (typically molecular line absorption or emission or/and reference blackbody radiation) and its IF converted signal are ordinarily three orders of magnitude below the local oscillator power. In this case, the dissipated power can be simplified to:

$$P_{\text{dissipated}} = \sum [P_{\text{LO input } hn}] \quad (2b)$$

In the present analysis, room temperature dissipated powers are calculated from measured values at first harmonic order using Equations (1a) and (2a) for frequency multipliers and mixer, respectively. They are simulated at cryogenic

temperature, using for the estimation of  $I_{DC}$ , Equations (1b) and (2b), with contribution of all unmatched frequency residuals. Those are strictly verified by harmonic balance simulation for a mixing order  $\geq 6$  (see Table II).

### B. Power dissipation budget

The design of the 300 GHz, 600 GHz doublers and 1200 GHz mixer have been developed for operation under room temperature conditions, i.e. 300 K [8], [19]. However, when lowering the physical temperature of operation, the thermal noise contribution decreases until the conduction is no longer dominated by thermionic emission but by quantum mechanics tunneling [34]. As the junction temperature drops even down to 120 K, the ideality factor of the junctions increases and their knee moves to higher voltage, boosting multipliers efficiency by a factor 1.5 to 2 depending on frequencies [35], [36]. This effect is usually advantageous to the systems. In our case it might lead to a risk in doubling the dissipated power per anode without proper control, and consequently higher up the risk of long-term degradation. Our methodology study consists in firstly assessing the maximum and best case dissipated limits from 300 K room temperature measurement including separated stages before final assembly of all components (paragraph IV.B.1), secondly assess that dissipation limits are kept below limits at 120-150 K temperature of operation (paragraph IV.B.2) despite limited programmatic time available at the time of final assessment.

#### 1. 300 K temperature operation

Fig.6 shows the set-up used for the RF measurements of the 1200 GHz receiver chain at 300K room temperature, conducted on FM and FSM chains during screening steps (health control) and also during pre-calibration test campaigns.

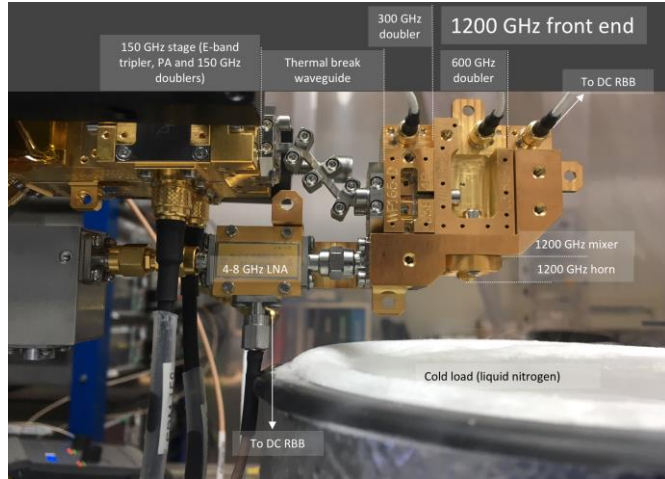


Fig. 6. Flight model of SWI 1200 GHz front-end during RF acceptance test (OBSPM-PSL premises) at 300 K room temperature before integration in the telescope and receiver unit (MPS premises).

The simulation consists in a co-simulation matching the integrated circuitry to a harmonic balance code provided by ADS. A 3D electromagnetic field simulator tool (High Frequency Structure Simulator) is used to calculate the passive scattering matrix of the diode geometry and its near field parasitic. This virtually duplicated geometry fits and defines the e-beam fabrication process, along with the micro-

mechanical waveguide structure [17],[33]. Room temperature measurement of the junction (IV) curve at DC (Table III) allows interpolation of the current equation [38] and approximate the junction parameters at 300 K as defined in [19],[35].

TABLE II

DC AND RF INDICATORS USED IN THE RETRO-MODELLING AT CRYOGENIC-TEMPERATURE.

\*D300 stands for 300 GHz doubler and D600 for 600 GHz doubler. RT is room temperature; CT is 120-150 K temperature.

	Temp.	Meas.	Retro-Model	Plot
$P_{IN}$ 150 GHz = $P_{IN}$ D300*	RT	✓		Fig. 7/ Fig.12 (a)
	CT	✓		Fig.12 (a)
$V_{DC}$ D300	RT	✓	from RT meas	
	CT	✓	from CT meas	
$I_{DC}$ D300	RT	✓	from RT meas	
	CT	✓	from CT meas	
$P_{DISS}$ D300	RT	Eq. (1a)	Eq. (1a) / Eq. 1b ( $I_{DC}$ )	Fig.13 (a) / Table IV
	CT	Eq. (1a)	Eq. (1a) / Eq. 1b ( $I_{DC}$ )	Fig.13 (a) / Table IV
$V_{SWING}$ D300	RT			
	CT			Fig. 14
$P_{OUT}$ D300 = $P_{IN}$ D600*	RT	✓		Fig. 7/ Fig. 12(b)
	CT	D300X1 only	Output of D300 modelling / Input to D600 modelling	Fig. 12(b)
$V_{DC}$ D600	RT	✓	from RT meas	
	CT	✓	from CT meas	
$I_{DC}$ D600	RT	✓	from RT meas	
	CT	✓	from CT meas	
$P_{DISS}$ D600	RT	Eq. 1(a)	Eq. (1a) / Eq. (1b) for $I_{DC}$	Fig. 13(b) / Table IV
	CT		Eq. (1a) / Eq. (1b) for $I_{DC}$	Fig. 13(b) / Table IV
$P_{OUT}$ D600 = $P_{OL}$ SHM1200	RT	✓		Fig. 7
	CT			
$V_{SWING}$ D600	RT	✓		
	CT		✓	Fig. 15
$V_{DC}$ SHM1200	RT	✓	from RT meas	
	CT	✓	from CT meas	
$I_{DC}$ SHM1200	RT	n/a	✓	
	CT	n/a	✓	
$P_{DISS}$ SHM1200	RT	Eq. 1(a)		Fig. 8
	CT		Eq. (1a) / Eq. (1b) for $I_{DC}$	Table IV

#### a) Multiplier case (300 K)

Previously, the output power levels, as well as DC rectified current values of the 300 GHz and 600 GHz doublers have been measured sequentially. Fig. 7 presents the measured and simulated output power levels as function of frequency. The input power for the 300 GHz doubler (which is the output power of the 150 GHz multiplier) is also presented for comparison. The dotted lines show the results of the retro-simulation performed using the measured values of frequency dependant DC voltage and diode parameters (see Table II).

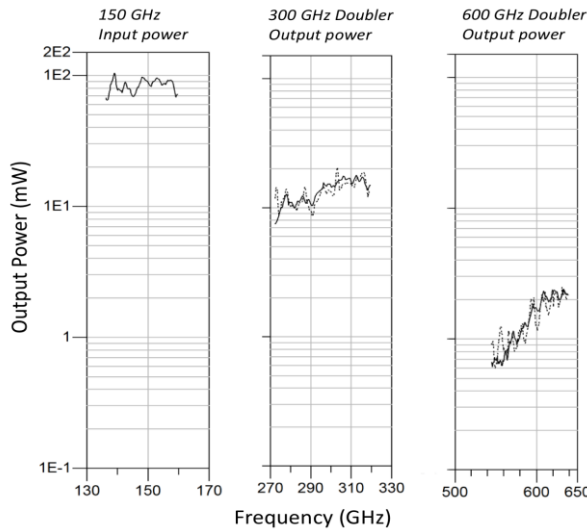


Fig. 7. The output powers of SWI FS 300 GHz and 600 GHz doublers measured during the acceptance phase at 300 K room temperature (bold-light represent measurement and dot-light represent retro-simulations).

b) Mixer case (300K)

Fig. 8 illustrates the measured performances (receiver noise temperature) versus LO frequency (Fig. 8(a)) and local oscillator power level (Fig. 8(b)) at 300 K room temperature across the full 1080-1280 GHz range. The cross markers correspond to the simulation of the mixer noise temperature at one central frequency  $f_{LO} = 585$  GHz, using the typical frequency-dependent DC bias (RBB levels) and local oscillator power values. As for the 300 GHz and 600 GHz frequency doublers, the junction parameters at 300 K are given by wafer values made during wafer screening and listed in Table III. The mixer activation point is defined by the DC bias voltage associated to the matched power of the local oscillator in mW at the two anti-parallel balanced Schottky mixer anodes.

Both measurement and simulation illustrate that the mixer performance improves by increasing the LO power level starting from zero up to a certain level, depending of the chosen working frequency. However, above this level, an additional increase of this LO power doesn't improve the performance, but rather increase the dissipated power at anode junction. Three zones of operation could be identified, going from maximum to minimum LO power level: i) Zone I covers the maximum LO power without activation of the mixer DC bias voltage ( $P_{LO} \geq 1$  to 2 mW), ii) Zone II covers the optimum operating point of the flight model and is centered around  $P_{LO} \in 0.75$ -1 mW and a DC bias voltage  $V_b \in 0$ -0.45 V at junction level (voltage across the two junctions in DC series), and iii) Zone III corresponds to acceptable performances with limited LO power ( $P_{LO} \leq 0.75$ mW). The Zone II - Zone III transition defines the edge of operating point ( $P_{LO} = 1$  mW and  $V_b = 0.25$  V), for keeping best performances with minimum LO power, thus minimum power dissipation. The tradeoff limits are obtained for 1 mW level, corresponding to 6 mW per  $\mu m^2$  per mixer anodes. These preliminary values are not yet representative to nominal 120-150 K temperature of operation, but exceeding of the level shall be prevented at cryogenic operation with limiting the RF tuning procedure. All the

measurements going above 6 mW per  $\mu m^2$  are translated into a thermal increase and subtracted in the expected life time of the herein FM chain (see part II).

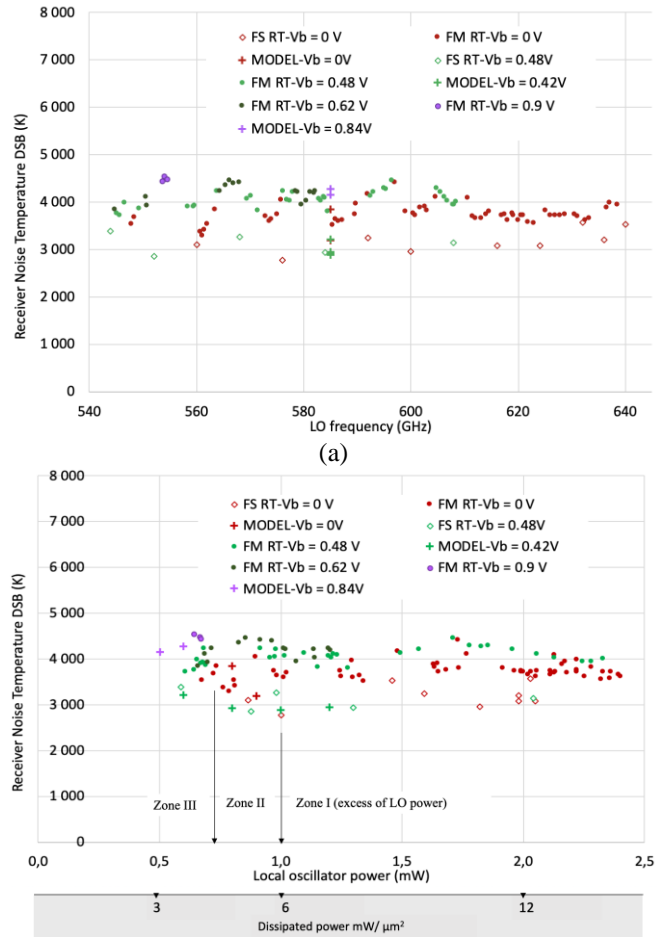


Fig. 8. Identification of operation of the 1200 GHz mixer at 300 K room temperature during acceptance (FM and FSM models): (a) versus LO frequency and (b) versus LO power sweep from 0.5 to 2.5 mW and equivalent dissipated power per junction area. All frequency points are given (from 1080-1280 GHz). DC voltages corresponds to RBB levels. Simulations are for  $f_{LO} = 585$  GHz only and are noted "MODE" (cross markers).

2. 120-150 K temperature operation

Fig. 9 shows the set-up inside the cryogenerator. The RF measurement of the flight model of the 1200 GHz cold electronic front-end were performed at cryogenic temperature with the 150 GHz stage flight models (provided by Radiometer Physics) and a Keysight/PSG Analog Signal Generator E8257D. Respectively, the front-end spare mode was tested with the 150 GHz Stage qualification model. The RF tests are conducted at 128 K and 158 K for the 1200 GHz cold electronic front-end and at 253 K and 273 K  $\pm 3$  K for the 150 GHz unit. 117 frequency points were optimized for the FM and 14 frequency points for the FSM chain during the pre-calibration campaign. For programmatic reasons, direct

cryogenic measurement of the efficiency at 300 GHz and 600 GHz could not be added as a separate step<sup>10</sup>.

Instead, the strategy of operation is defined by transition procedures between state mode of the instrument to secure any failure of the junctions [37], [31] and confirmed with simulation.

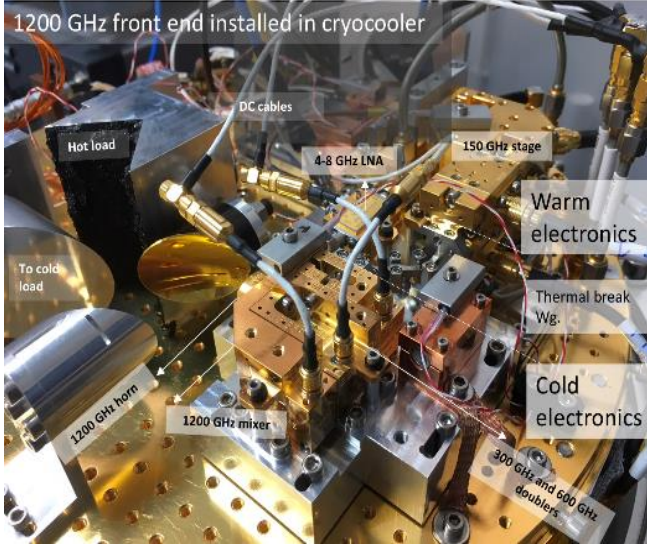


Fig.9. The RF acceptance test set-up performed at OBSPM-PSL on FM models.

Firstly, the experimental procedure is divided in three progressive steps for securing safe operation of the Schottky junctions while reaching optimum DC-bias values. The starting

condition is that the synthesizer is in standby and all receiver unit components are OFF. In a first step, and before enabling the attenuation level of the K-band synthesizer output, the 300 GHz and 600 GHz doublers are DC biased with value set by the look up table, previously defined in [15]. During this step, the mixer DC voltage is DC grounded through the RBB inhibited port. In a second step, the K-band synthesizer output power is set to a minimum value then the bias voltage of each frequency doubler of the local oscillator are adjusted sequentially and for maximum mixing efficiency until the best noise temperature has been reached. Finally, the mixer DC tuning is activated if necessary in a third step. Any decrease in receiver performance revert the operation to previous tuning steps, thus forcing a one-way iteration of the optimization.

Secondly, three retro-simulations are necessary for the complete cryogenic assessment of dissipated power of the junction used in the 1200 GHz cold electronic chain. The 300 GHz doublers MMIC circuit retro-models at 120-150 K temperature (output power) is used as input to 600 GHz retro-modelling, used subsequently as an input to the 1200 GHz retro-modelling. The available measured values (Table II) are the input power at the 150 GHz stage and every frequency-dependent DC bias tunings and DC rectified currents. Other indicators were assessed through simulation. In addition, the junction DC (IV) curves performed at cryogenic temperatures (Fig. 11 and Table II) and allow to interpolate the current equation [38] and approximate the junction parameters at 150 K as defined in [35]. The results of the three-steps simulation is sufficient for the power density assessment and optimization (pre-calibration campaign). The extension of the simulation consists in modelling the full chain (i. e with merged three simulation steps) that could be used as an input to the

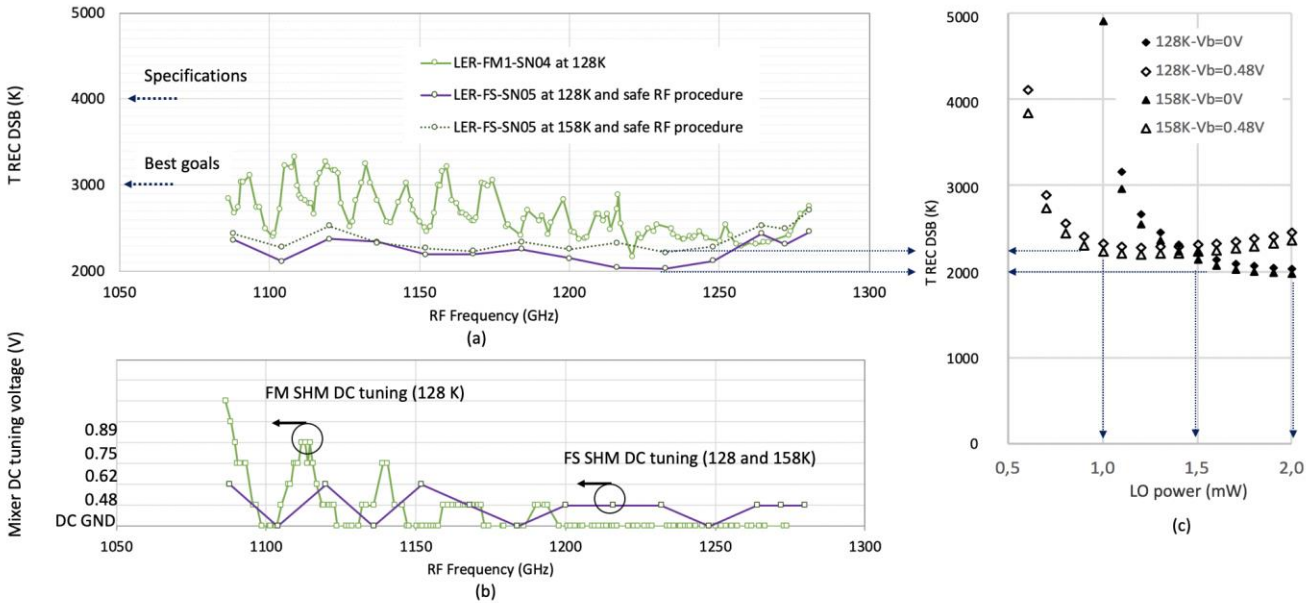


Fig. 10. Safe tuning algorithm and its impact on noise performances for FM models. (a) 1200 GHz front-end performance at 120-150 K room temperature (FS models) and (b) Simulation frequency is 1200 GHz, estimation of DSB receiver noise temperature versus local oscillator power level. This result allows to significantly flatten the noise performance over the full bandwidth<sup>11</sup>.

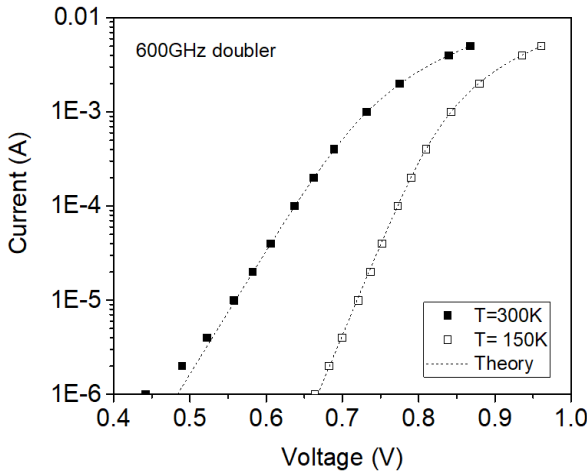
<sup>10</sup> except for the single chip 300 GHz doubler as part of SWI- 600 GHz channel.



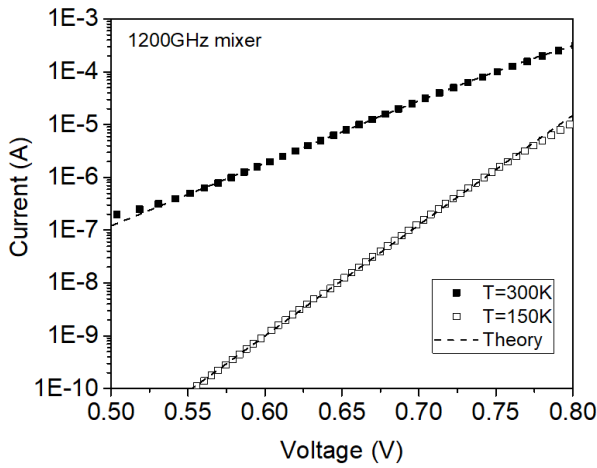
calibration campaign spurious modelling analysis <sup>11</sup>.

Fig. 10 (a) shows the DSB noise temperature measurement at 128 and 158 K for the flight spare model at different frequencies. Fig. 10 (b) is the corresponding modelling for different local oscillator power level sweep from 0.5 to 2 mW. The DC tuning of the mixer is activated at minima, always going from Zone II to Zone III states. Therefore, safe RF optimization during acceptance tests allows to keep below a maximum of 2 mW dissipated power for the two-anode mixer chip, while improving the performances. In Fig. 12, we demonstrate that the safe RF tuning mentioned earlier has the effect to limit the power levels despite cryo-cooling [36].

Fig. 13 gives the dissipated powers per anode (expressed in mW per  $\mu\text{m}^2$ ), for the 300 GHz and 600 GHz doublers. They are calculated using Eq. (1a) with measured values (RF input and output powers, DC voltages and DC rectified current at every tuning frequency) and Eq. (1b) for the estimation of  $I_{DC}$ .



(a)



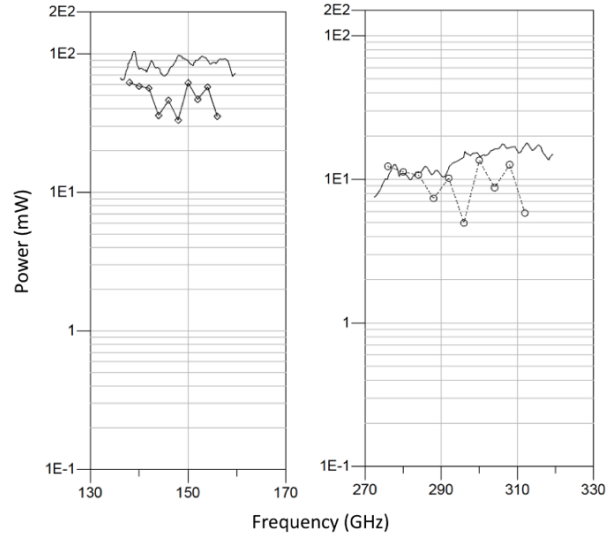
(b)

Fig. 11. IV characteristics measured (a) on 600 GHz doubler and (b) on 1200 GHz mixer at 150K (white squares) and 300 K (black squares). The dashed line is the theoretical fit [19][38].

TABLE III

DIODES DC PARAMETERS

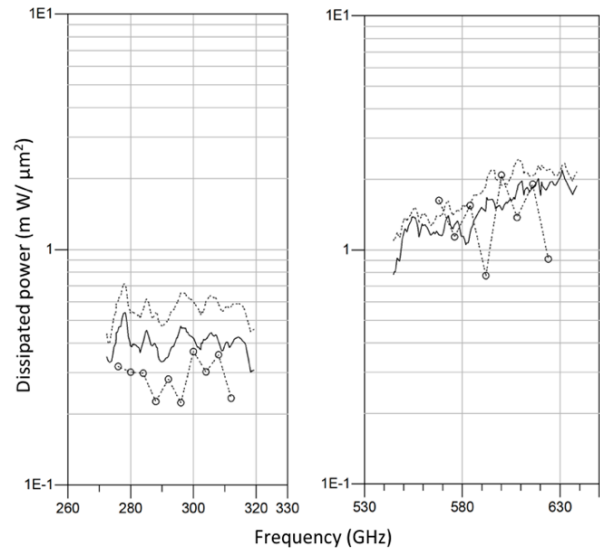
Diodes	Temp	$R_s$ ( $\Omega$ )	$C_{j0}$ (fF)	$\eta$	$I_s$ (A)
300 GHz	300 K	7	18.5	1.21	$2.36 \times 10^{-12}$
	150 K	6	18.5	1.59	$2.45 \times 10^{-22}$
600 GHz	300 K	21	4.5	1.23	$1.75 \times 10^{-13}$
	150 K	20	4.5	1.77	$2.01 \times 10^{-21}$
1200 GHz	300 K	53	0.5	1.4	$0.5 \times 10^{-11}$
	150 K	53	0.5	1.5	$1 \times 10^{-22}$
	128 K	53	0.5	1.6	$1 \times 10^{-25}$



(a)

(b)

Figure 12: (a) Measured input powers before the 150 GHz thermal break titanium waveguide (300K: bold-light, 150K: bold-circle), (b) Measured and simulated power at 300 GHz (300K measurement: bold-light, 150K simulation: bold-circle).



(a)

(b)

Figure 13: Dissipated power per anode area in  $\text{mW per } \mu\text{m}^2$  for the (a) 300 GHz doubler and (b) 600 GHz doubler (300K measurement: bold-light, 300K simulation: dot-light, 150K simulation: dot with circle).

<sup>11</sup> See further publications on SWI in “Space Science Review Paper”.

TABLE IV  
DISSIPATED POWER

Dissipated power per junction area		300 K		120-150 K	
		AIT/AIV screening		AIT/AIV acceptance	
		in mW/ $\mu\text{m}^2$	in mW/ $\mu\text{m}^2$	Temp.increase (K) ( $R_{th}=3000\text{-}5000\text{ K/W}$ )	
				Per anode	Per chip
300 GHz	Avg.	0.4	0.3	19	36
	Max	0.6	0.4	32	128
600 GHz	Avg.	1	1	26	52
	Max	3	3	44	88
1200 GHz	Avg.	0.7	3	3	6
	Max	12 <sup>1</sup>	6	5	10

V. DISCUSSION

The maximum allowed dissipation power per Schottky junctions, expressed in mW per  $\mu\text{m}^2$  are the maximum of the junction power budget assessed during operation with the one-way tuning algorithm for safe RF operation. For the multiplier’s operation, excess in voltage swing is simulated and illustrated in Fig. 14 and 15. The zone of negative DC current is not recommended. The first and practical recommendation to avoid reverse current is to keep the minimum value of the DC rectified current always positive. For the mixer operation, the DSB noise temperature performances of the 1200 GHz chain are reached with an identified minimum LO power (Fig. 10), with a uniquely flat level over the full 1080-1280 GHz bandwidth. The junction temperature increase is calculated using the parameters from [39], [40]. It is summarized in Table IV as maximum dissipated power per junction area, and serves as an input to part II, to demonstrate long life operation and critical failure margins.

In this paper we have shown that the DC tuning allows to ensure very good performances over a wide RF bandwidth of 20%. Good performances can be maintained even at the band edges where the LO power falls to very low levels. Once the observing frequency has been selected, the DC bias of the LO and mixer is kept constant and therefore should not impact the stability of the receiver. A full characterization including linearity, stability, IF band characteristics and side band ratio has been carried out at MPS after the receiver had been fully integrated. The results of these measurements will be presented by *Hartogh et al.* that will be published very soon.

In part II, we put in perspective reliability during operation, endurance testing and determine allowed tuning deviations. Firstly, the  $P_{LO} = 1\text{ mW}$  and  $V_b = 0.25\text{ V}$  turn on point is used for RF endurance testing of the full 1200 GHz chain at 300 K (RF accelerated life tests). Secondly, DC endurance testing allows to push the dissipation power level according to Table IV.

ACKNOWLEDGMENT

The authors want to thank R. Moreno from LESIA Observatoire de Paris PSL, J-L. Roux, from CNES, C. Berthod and J. Spatazza from CNRS-INSU, D. Moirin, from Hensolt Space Consulting, T. Galtier, O. Mbeumou, and V. Leray from Nexeya Space Consulting, M. Gregoire from Logical and J-L. Espagnol from Bureau Veritas. The work includes the

participation of partners and companies, amongst them are Syrlinks, SAP, Kerdy, RPG and the SWI consortium.

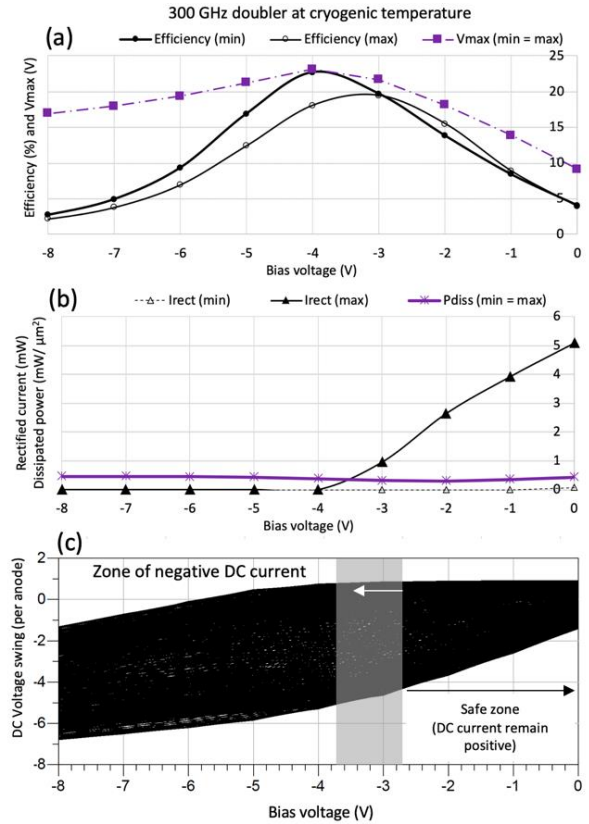


Figure 14: 300 GHz frequency dual chip doubler operation at 150 K, as a function of total DC bias.: (a) minimum and maximum efficiency, maximum voltage, (b) minimum and maximum rectified current, Dissipated power, (c) Vpeak per anodes Zones.

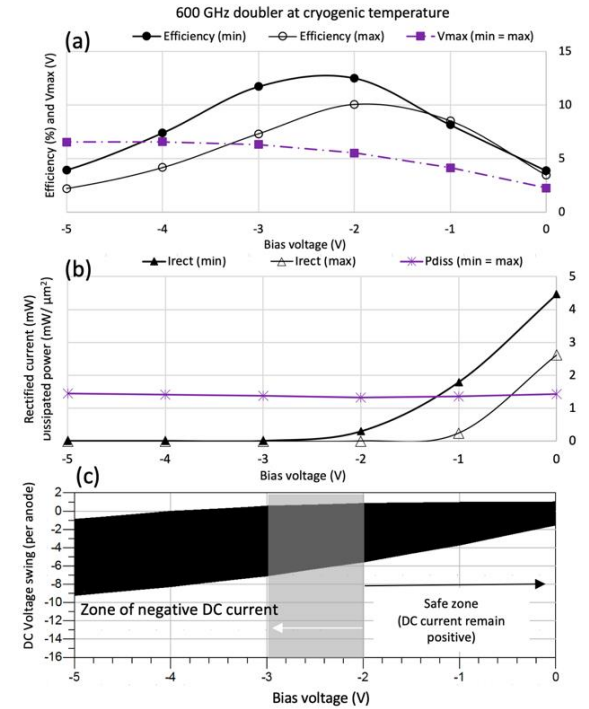


Figure 15: 600 GHz frequency dual chip doubler operation at 150 K, as a function of total DC bias.: (a) minimum and maximum efficiency, maximum

voltage, (b) minimum and maximum rectified current, Dissipated power, (c) V<sub>peak</sub> per anodes Zones.

## REFERENCES

- [1] Max Planck Institute für Solar System Research. <https://www.mps.mpg.de/planetary-science/juice-swi>
- [2] P. Hartogh “The Submillimetre Wave Instrument (SWI) on JUICE,” in preparation (SSRv 2023).
- [3] G. K. Hartmann, R. M. Bevilacqua, P. R. Schwartz, N. Kämpfer, K. F. Künzi, C. P. Aellig, A. Berg, W. Boogaerts, B. J. Connor, C. L. Croskey, M. Daehler, W. Degenhardt, H. D. Dicken, D. Goldizen, D. Kriebel, J. Langen, A. Loidl, J. J. Olivero, T. A. Pauls, S. E. Puliafito, M. L. Richards, C. Radian, J. J. Tsou, W. B. Waltman, G. Umlauf, R. Zwick, “Measurements of O<sub>3</sub>, H<sub>2</sub>O and ClO in the middle atmosphere using the millimeter-wave atmospheric sounder (MAS)” *Geophysical research Letters*, Volume 23, Issue 17, pp. 2313-2316, Aug. 1996 doi: [10.1029/96GL01475](https://doi.org/10.1029/96GL01475).
- [4] C. L. Croskey, N. Kämpfer, R. M. Belivacqua, G. Karlheinz Hartmann, K. F. Kunzi, Philip R. Schwartz, J. J. Olivero, S. E. Puliafito, C. Aellig, G. Umlauf, W. B. Waltman, and W. Degenhardt, “The millimeter wave atmospheric sounder (MAS): a shuttle-based remote sensing experiment”, *IEEE Microwave Theory and Tech.*, vol. 40, no. 6, pp. 1090-1100, June 1992, doi: [10.1109/22.141340](https://doi.org/10.1109/22.141340).
- [5] U. Frisk et al. “The Odin satellite - I. Radiometer design and test”, *A&A*, 402 3 (2003) L27-L34, doi: [10.1051/0004-6361:20030335](https://doi.org/10.1051/0004-6361:20030335).
- [6] S. Gulkis, M. Frerking, J. Crovisier, et al. “MRO: Microwave Instrument for Rosetta Orbiter”, *Space Sci. Rev.*, vol. 128, pp. 561–597, 2007, doi: [10.1007/s11214-006-9032-y](https://doi.org/10.1007/s11214-006-9032-y).
- [7] De Graauw et al. “The Herschel-Heterodyne Instrument for the Far-Infrared (HIFI)”, *Astronomy and Astrophysics*, vol. 518, id. L6, July 2010, doi: [10.1051/0004-6361/201014698](https://doi.org/10.1051/0004-6361/201014698)
- [8] A. Maestrini, L. Gatilova, J. Treuttel, F. Yang, Y. Jin, A. Cavanna, D. Moro Melgar, F. Tamazouzt, T. Vacelet, A. Féret, F. Dauplay, J.-M. Krieg, C. Goldstein, “1200GHz and 600GHz Schottky receivers for JUICE-SWI”, in *Proc. of the 27th International Symposium on Space Terahertz Technology*, 3 pages, 12-15 April 2016, Nanjing, China.
- [9] A. Maestrini et al., “The 1200GHz Receiver Front-end of the Submillimetre Wave Instrument of ESA Jupiter ICy moons Explorer,” *2018 43rd International Conference on Infrared, Millimeter, and Terahertz Waves (IRMMW-THz)*, Nagoya, Japan, 2018, pp. 1-2, doi: [10.1109/IRMMW-THz.2018.8509935](https://doi.org/10.1109/IRMMW-THz.2018.8509935).
- [10] K. Jacob et al., “Characterization of the 530 GHz to 625 GHz SWI receiver unit for the Jupiter mission JUICE,” in *Proc. 36th ESA AntennaWorkshop*, Noordwijk, The Netherlands, 2015, pp. 1–6.
- [11] M. Kotiranta, K. Jacob, H. Kim, P. Hartogh, A. Murk, “Optical Design and Analysis of the Submillimeter-Wave Instrument on JUICE”, *IEEE Transactions on Terahertz Science and Technology*, vol. 8, no 6, pp. 588-595, Nov. 2018, doi: [10.1109/TTHZ.2018.2866116](https://doi.org/10.1109/TTHZ.2018.2866116)
- [12] H.J. Gibson, B. Thomas, L. Rolo, M. C. Wiedner, A. Maestrini, P.de Maagt, “A novel spline-profile diagonal horn suitable for integration into THz split-block components”, *IEEE Transactions on Terahertz Science and Technology*, vol. 7, no. 6, pp. 657-663, Nov. 2017, doi: [10.1109/TTHZ.2017.2752423](https://doi.org/10.1109/TTHZ.2017.2752423)
- [13] J.L. Besada, “Influence of local oscillator phase noise on the resolution of millimeter-wave spectral-line radiometers,” *IEEE Trans. Instr. Meas.*, vol. IM-28, no. 2, June 1979.
- [14] J. Treuttel, L. Gatilova, F. Yang, A. Maestrini, Y. Jing, A. Cavanna, T. Vacelet, F. Tamazouzt, and J.-M. Krieg, C. Goldstein., “A 330 GHz frequency doubler using european MMIC Schottky process based on e-beam photolithography, General Assembly and Scientific Symposium, XXXIth (URSI GASS), Beijing, China., Aug. 2014, doi: [10.1109/URSIGASS.2014.6929454](https://doi.org/10.1109/URSIGASS.2014.6929454)
- [15] A. Maestrini et al., “The 1200GHz receiver front-end of the Submillimeter Wave Instrument of ESA Jupiter ICy moons Explorer” , presented on *8th ESA Workshop on Millimetre-Wave Technol. Appl.*, ESA/ESTEC, Noordwijk, The Netherlands, Dec. 2018.
- [16] E. Schlecht, “Wide-band heterodyne submillimeter wave spectrometer for planetary atmosphere”, in *Proc. of 21st International Symposium on Space THz Technol.* Oxford, England, March 2010.
- [17] J. Treuttel et al., “A 520–620-GHz Schottky Receiver Front-End for Planetary Science and Remote Sensing With 1070 K–1500 K DSB Noise Temperature at Room Temperature”, *IEEE Trans. THz Sci. Technol.*, vol. 6, no. 1, pp. 148-155, Jan. 2016, doi: [10.1109/TTHZ.2015.2496421](https://doi.org/10.1109/TTHZ.2015.2496421)
- [18] L. Gatilova, A. Maestrini, J. Treuttel, T. Vacelet, Y. Jin, A. Cavanna, L. Coureaud, A. Féret, G. Gay, S. Caropen, J. Valentin, S. Mignoni, J.-M. Krieg, C. Golstein, “Recent progress in the development of french THz Schottky diodes for astrophysics, planetology and atmospheric study”, in *Proc. of 44th International Conference on Infrared, Millimeter, and Terahertz Waves (IRMMW-THz)*, Paris, France, Sep. 2019, doi: [10.1109/IRMMW-THz.2019.8873728](https://doi.org/10.1109/IRMMW-THz.2019.8873728).
- [19] J. Treuttel, T. Thuroczy, A. Feret, G. Gay, L. Gatilova, T. Vacelet, C. Chaumont, E. Sernoux, P. Mondal, J. Puech, “Demonstration of a 25% bandwidth 520-680 GHz Schottky receiver front-end for planetary science and remote sensing,” *Proc. SPIE* 12190, Millimeter, Submillimeter, and Far-Infrared Detectors and Instrumentation for Astronomy XI, 121902Y, Aug. 2022, doi: [10.1117/12.2630052](https://doi.org/10.1117/12.2630052).
- [20] P. Bertram, « Développement de l'instrument heterodyne MIRO pour la sonde cometaire Rosetta de l'ESA, » PhD, Univ. Paris 6, France, 1999
- [21] G. Chattopadhyay, E. Schlecht, F. Maiwald, R. Dengler, J. Pearson and I. Mehdi, “Frequency multiplier response to spurious signals and its effect on local oscillator systems in millimeter and submillimeter wavelengths”, in *Proc. of SPIE, Millimeter and Submillimeter Detectors for Astronomy*, vol. 4855, pp. 480–488, Feb. 2003, doi: [10.1117/12.459195](https://doi.org/10.1117/12.459195).
- [22] J.T. Louhi, A.V. Raisanen, and N. R. Erickson “Cooled Schottky varactor frequency multipliers at submillimeter wavelengths”, *IEEE MTT*, vol. 41, no. 4, pp. 565-571, Apr. 1993, doi: [10.1109/22.231647](https://doi.org/10.1109/22.231647).
- [23] H. M. Pickett, R. L. Poynter, E. A. Cohen, M. L. Delitsky, J. C. Pearson, and H. S. P. Muller, “Submillimeter, Millimeter, and Microwave Spectral Line Catalog,” *J. Quant. Spectrosc. & Rad. Transfer* 60, 883-890 (1998).
- [24] C. P. Endres, S. Schlemmer, P. Schilke, J. Stutzki, and H. S. P. Müller, The Cologne Database for Molecular Spectroscopy, CDMS, in the Virtual Atomic and Molecular Data Centre, *VAMDC J. Mol. Spectrosc.* 327, 95–104 (2016)
- [25] A. Grüb-, Krozer, A. Simon and H. L. Hartnagel, “Reliability and microstructural properties of GaAs Schottky diodes for submillimeter-wave applications”, *Solid-State Electronics* , Vol. 37, No. 12, pp. 1925-1931, 1994
- [26] M. C. Casey, J.-M. Lauenstein, R. A. Gigliuto, E. P. Wilcox, A. M. Phan H. Kim, D. Chen, and K. A. LaBel, “Destructive Single-Event Failures in Schottky Diodes”, *Electronics Technology Workshop (ETW)*, Greenbelt, MD, June 2014.
- [27] M. C. Casey, J.-M. Lauenstein, E. P. Wilcox, A. D. Topper, M. J. Campola, and K. A. LaBel, “Failure Analysis of Heavy-Ion-Irradiated Schottky Diodes”, *NASA Goddard Space Flight Center, Code 561.4, Greenbelt, MD 20771 AS&D, Inc., Seabrook, MD 20706*.
- [28] T. Wilcox, M. Campola, M. Joplin, “Single-Event Effect Test Report International Rectifier 80SCLQ060SCS Schottky Diode”, Feb 2021, *NASA Goddard Space Flight Center, Greenbelt, MD USA*.
- [29] R. Lin I. Mehdi, A. Pease, R. Dengler, D. Humphrey, T. Lee, A. Scherer, and S.Kayali “Accelerated lifetime testing and failure analysis of quartz based GaAs planar Schottky diodes”, in *Proc. of 1997 GaAs Reliability Workshop.*, Anaheim, CA, USA, Oct. 1997, pp. 19-39, doi: [10.1109/gaasrw.1997.656117](https://doi.org/10.1109/gaasrw.1997.656117).
- [30] F. Maiwald, E. Schlecht, R. Lin, J. Ward, J. Pearson, P. Siegel, and I. Mehdi “Reliability of cascaded THz frequency chains with planar GaAs circuits”, in *Proc. of 15th International Symposium on Space THz Technol.*, Apr. 2004, Northampton, Massachusetts, USA, pp. 128-134.
- [31] F. Maiwald, E. Schlecht, J. Ward, R. Lin, R. Leon, J. Pearson. and I. Mehdi “Design and operational considerations for robust planar GaAs varactors: A reliability study”, in *Proc. of 14th ISSTT*, Pasadena, CA, USA, Apr. 2003.
- [32] S. Maas, *Nonlinear microwave and rf circuits*, 2<sup>nd</sup> ed. Norwood, MA, USA, Artech House, 2003, pp. 582.
- [33] Maestrini, A., B. Thomas, H. Wang, C. Jung, J. Treuttel, Y. Jin, G. Chattopadhyay, I. Mehdi, and G. Beaudin, “Schottky diode based terahertz frequency multipliers and mixers”, invited paper, *Comptes Rendus de l'Académie des Sciences, Physique*, vol. 11, no. 7-8, August-October 2010, doi: [10.1016/j.crhy.2010.05.002](https://doi.org/10.1016/j.crhy.2010.05.002).
- [34] F. Padovani, A. Stratton, “Field and Thermionic Field Emission in Schottky Barriers”, *Solid-State Electronics*, Pergamon Press 1966. Vol. 9, pp. 695-707, doi: [10.1016/0038-1101\(66\)90097-9](https://doi.org/10.1016/0038-1101(66)90097-9).

- [35] E. Schlecht, F. Maiwald, G. Chattopadhyay, S. Martin, I. Mehdi, "Design considerations for heavily-doped cryogenic Schottky diode varactor multipliers", in *Proc. of 12th International Symposium on Space Terahertz Technology*, San Diego, California, Feb. 2001, pp. 485-494.
- [36] A. Maestrini, D. Pukala, E. Schlecht, I. Mehdi and N. Erickson, "Experimental investigation of local oscillator chains with GaAs planar diodes at cryogenic temperatures", in *Proc. of the 12th International Symposium on Space Terahertz Technology*, San Diego, USA, Feb. 2001, pp. 495-503
- [37] M.Ciechanowicz and T.Klein, "Hershell report HIFI - LO LO/SS operation" Max Planck Institute für radioastronomie, MPIfR/HIFI/TN/2001-521, Oct. 2006
- [38] E. L. Kollberg, T. J. Tolmunen, M. A. Frerking, and J. R. East, "Current saturation in submillimeter wave varactors," *IEEE Trans. Microwave Theory Tech.*, vol. 40, no. 5, 1992, pp. 831-838, doi.: [10.1109/22.137387](https://doi.org/10.1109/22.137387).
- [39] S. Adachi, "GaAs and related materials: bulk semiconducting and superlattice properties", Gunma Univ., Japan, World Scientific, 1994, pp. 696, doi.: [10.1142/2508](https://doi.org/10.1142/2508)
- [40] A. Y. Tang, E. Schlecht, G. Chattopadhyay, R. Lin, C. Lee, J. Gill, I. Mehdi and J. Stake, "Steady-State and Transient Thermal Analysis of High Power Planar Diodes", in *Proc. of 22<sup>nd</sup> International Symposium on Space Terahertz Technology*, Tucson, Arizona, USA, Apr. 2011.



**J. Treuttel** Dr. received in 2011 the Ph.D. degree in Instrumentation for Astronomy and Astrophysics from the Observatory of Paris and Centre National d'Etudes Spatiales (CNES), strongly associated with the Rutherford Appleton Laboratory, UK. In 2010 she joined permanently the Observatory of Paris, as engineering scientist, and has designed state-of-the-art III-V Schottky mixers and multipliers. In 2015 she received a NASA Postdoctoral Fellowship grant to work at the Jet Propulsion Laboratory on the development of the first all-solid-state 2 THz heterodyne receiver with the JPL-MDL Schottky technology. Back at Observatoire de Paris PSL in 2018, she endorsed the role of system engineer for the Submillimeter Wave Instrument 1200 GHz front-end as a major (French) contribution to the Jupiter JUICE-L1 ESA mission. Her current research interests are in the design of integrated THz electronics MMIC and systems for radio astronomy and planetary science space missions. She is working in close partnership with CNRS-Centre de Nanostructures et Nanotechnologies and Institut d'Electronique de Microélectronique et de Nanotechnologie for the development of Schottky diode processes and their qualification for operational space instrumentation up to several THz.



**L. Gatilova** Dr. received in 2007 the PhD degree in physics from the University Paris XI, Orsay, France. Up to 2013 she worked as engineering scientist on dry etching plasma applications for III-V semiconductors at Laboratoire de Photonique et Nanostructure, Marcoussis, France. Since 2013 she permanently joined Observatoire de Paris as research engineer and is responsible for the development and fabrication of micro- and nanoelectronic devices based on Schottky diode technologies. This work is conducted in the clean room of CNRS- Centre de

Nanostructures et Nanotechnologies, France in close collaboration with Observatoire de Paris-PSL. Her research interests are focused on the development of nanotechnologies in order to realize high performance submicron Schottky diodes and the diodes-based circuits for sub-THz and THz applications, as well as their qualification for high TRL space application.



**Sylvain Caroopen**, MsC. Sylvain Caroopen received in 2000 the Engineering degree in microwaves and space telecommunications from the Conservatoire des Arts et Métiers in Paris, France. Since 2000, he has been with the THz region for more than 20 years dealing with VNA driving THz sources and mm/submm receivers, since 2016 CEO of AB Millimètre company, recently started to work on space projects dealing with TWT/ SSPA RF amplifiers.



**A. Feret** obtained his MsC degree at the University of Lille 1 in 2001 in microwave microelectronics. He is involved in the development, with strong focus on testing and characterization of SIS junctions, HEB and Schottky diodes for THz heterodyne receivers dedicated to radio astronomy at CNRS-Observatoire de Paris, PSL. He is currently responsible of the microwave laboratory measurement benches. He received in 2008 together with the SIS project team the Conseil National des ingénieurs et Scientifiques de France engineering award for his work on the qualification and integration of SIS mixers of the Channel 1 Herschel - HIFI instrument, and was highly involved in technical contribution for the Submillimeter Wave Instrument for the Jupiter JUICE-L1 ESA mission during development and pre-calibration measurement phase.

**Gregory Gay**, Dr. received a PhD degree in electronics from the Université Pierre et Marie Curie-Paris VI, France, in 2013. From 2013 to 2016, he was an Engineering scientist in Observatoire de Paris, working on hot-electron bolometers in the Laboratoire d'Etude du Rayonnement et de la Matière en Astrophysique (LERMA). From 2016 to 2021, he has been a member of the team working on the ESA's space mission Jupiter ICy moons Explorer (JUICE).



**Jérôme Valentin**, Dr. received the Master of Engineering degree in physics engineering and the Ph.D. degree in physics from the Institut National des Sciences Appliquées, Toulouse, France, in 2000 and 2004, respectively. He was an Engineer in the field of semiconductor devices microfabrication and characterization. At Procion analysis, he worked on semiconductor characterization by Secondary Ion Mass Spectroscopy. He gained fabrication and process development

experience at several French technological platforms (LAAS, FEMTO-ST, Minatech PTA, C2N). Since 2018, he has been a Permanent CNRS Research Engineer with the Laboratoire d'Etude du Rayonnement et de la Matière en Astrophysique et Atmosphères, Observatoire de Paris, Paris, France. He participated in the Schottky diodes chips fabrication for the SWI instrument of JUICE ESA's mission and was involved in their spatial qualification process. He is currently working on instrumental projects in the field of THz heterodyne detection.



**A. Cavanna** is research engineer at CNRS since 1994. Her main activity consists in the growth of III-V compound semiconductors by MBE (Molecular Beam Epitaxy), such as heterojunctions for two-dimensional electron gas, tunneling diodes, quantum cascade laser. Her other activity concerns on the graphene synthesis by Chemical Vapor Deposition and their report process.



**Thibaut Vacelet** is an Engineer with LERMA, Observatoire de Paris, France. He is responsible for the microassembly and integration activities of devices dedicated to THz heterodyne instruments, including SIS and HEB mixers, Schottky mixers and frequency multipliers.



**Y. Jin Dr.** is research director at CNRS. He has developed specific process for realizing nanostructured field-effect devices for fundamental and applied physics. He has scientific, technical and administrative responsibilities in five European research programs and more than ten French national research projects on topics of hyper-frequency HEMTs, Coulomb blockade, quantum shot noise reduction, fractional charge  $e/3$  by shot noise, mesoscopic circuits and cryogenic electronics. His current research interests include quantum coherent mesoscopic circuits, a new generation of ultra-low noise HEMTs for low frequency high impedance deep cryogenic readout electronics and nano-Schottky diodes for sub-THz and THz space electronics.



**K. Jacob, Dr.** received the M.Sc. degree in physics from the Albert Ludwigs University of Freiburg im Breisgau, Freiburg im Breisgau, Germany, in 2014, and the Ph.D. degree in physics from the University of Bern, Bern, Switzerland, in 2018. From 2014 to 2020, he was with the Institute of Applied Physics, University of Bern, Bern, Switzerland, and from 2020 to 2021, he was with the Max Planck Institute for Solar System Research, Göttingen, Germany, where he worked on the development and characterization of submillimeter-wave instrumentation. Since 2021, he has been with Armasuisse Science and Technology, Thun, Switzerland, where he works on electromagnetic

compatibility, high-power electromagnetics, and nonionizing radiation studies with the Swiss NEMP Laboratory, Spiez.



**S. Mignoni**, PhD in Optics, was Project Manager at LERMA for the JUICE-SWI instrument. She worked at Observatoire de Paris with the THz heterodyne team in order to provide Schottky mixers and frequency multipliers for spatial use.



**V. Lavignolle**, MsC. has an extensive experience of the Aerospace & Military industry. He joined Airbus Defense & Space in 1995 (formerly EADS Astrium) and held leadership roles across engineering, operations, program management, including International R&D Programs. Later, he joined Upgrade and Aircraft Retrofit Programs in Dassault and Air France Industrial Directorates. He was also involved in Certification and Airworthiness challenges for Annex II Aircraft and Unmanned vehicles. Since the 2010's, he served on various Board of Directors and SME's corporate governances as a Space Technical Advisor. More recently he is contributing to CNES & CNRS French leading projects and R&D Programs supporting Phases B/C/D. He is associate member of IHEDN and served as reservist in the French Army.

**J-M. Krieg**, received the M.Sc. degree in engineering from the École nationale supérieure de mécanique et des microtechniques, Besançon, France, in 1983, and the Ph.D. degree in electronic engineering from the University of Franche-Comté, Besançon, France, in 1987 with a work on microwave oscillators. From 1987 to 1996, he was with Thales Electronic Devices as a Research Engineer. He then joined the Observatoire de Paris, where he was involved in several space projects, such as ROSETTA-MIRO, HERSCHEL-HIFI, and JUICE-SWI.

**C. Goldstein**, photograph and biography not available at the time of publication.



**F. Courtade**, MsC. is Currently Head of « mechanisms & AOCS equipments » office at CNES Toulouse space Center. He has joined CNES in 1991 and take over the in-house expertise lab for technology and failure analysis of Electronic Electromagnetic and Electrical Components. He is expert in Component technology for Hirel an COTS, he joined the PURE® team for provider assessment worldwide. Then he led many research technology studies in the field of MEMS and other micro and nanotechnology-based devices. From 2014 to 2020 he became Instrument manager of the French contribution to the JUICE (Jupiter Icy Moon Explorer) payload and led the French Research & technology program for the development of

advanced scientific instruments for planetology and exobiology exploration.

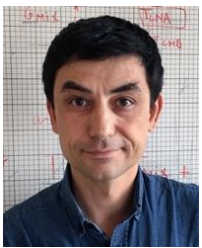


**C. Larigauderie**, is at CNES since 1990 after 5 years in aeronautic industry. She had made several duties as computer science engineer, on-board software engineer, instrument responsible and she managed several space projects, the last one is Project manager of French contributions to JUICE. She is now Deputy Head of Space Science Projects at CNES.



**A. Ravanbakhsh**, Dr. received the M.Sc. in aerospace engineering in 2005 from the Amirkabir University of Technology in Teheran, Iran. In 2010 and 2014 he received the M.Eng. and Dr.Eng. respectively in aerospace engineering from the Universidad Politécnica de Madrid (UPM), Spain. He worked as system engineer and AIVT manager of the Electron Proton Telescope (EPT), High Energy Telescope (HET), and SupraThermal Electrons, Proton (STEP) from the Energetic Particle Detector (EPD) consortium of the ESA Solar Orbiter mission at the University of Kiel, Germany. At Kiel University he provided support in thermal/structural engineering for the Chinese Chang'e-4 Moon lander mission and was involved as project manager and system engineer in the ESA Lagrange mission. Since 2020 he works as an AIVT manager and project manager for the JUICE Submillimetre Wave Instrument at MPS, Göttingen, Germany.

**J-P. Garcia**, photograph and biography not available at the time of publication.



**A. Maestrini** Dr. received the M.S. degree in telecommunications and electrical engineering from the Ecole Nationale Supérieure des Télécommunications de Bretagne, France, in 1993. From 1993 to 1995, he was an RF Engineer with the Receiver Group, IRAM 30-m Telescope, Spain. In 1999, he received the Ph.D. degree in electronics jointly from the Université de Bretagne Occidentale and the Observatoire de Paris, France. In 1999, he joined the Submillimeter-Wave Advanced Technology (SWAT) Group at the Jet Propulsion Laboratory, California Institute of Technology, USA, where he was involved in solid-state terahertz (THz) local oscillator development for the heterodyne instrument (HIFI) for the Herschel Space Observatory. In 2002, he returned to the Observatoire de Paris PSL, LERMA, and joined the Sorbonne Université, Paris, as an Associate Professor in electronics and microwaves. In 2009, he received the Arago award from the French Academy of Sciences for his work on the local oscillators of Herschel-HIFI. He has been the Scientific Leader with the THz Instrumentation Group, from

2012 to 2019. His research focused on THz electronic sources and mixers for space applications. From 2013 until 2019, he led the French hardware contribution to the Submillimeter Wave Instrument (SWI) for ESA JUpier ICy moons Explorer that included the 1200GHz Schottky sub-harmonic mixer and the submillimeter wave frequency multipliers. Since 2013 he is a Co-Investigator of SWI. In 2019 he returned to the SWAT team at the Jet Propulsion Laboratory where he is now a senior RF engineer. His current research focusses on millimeter-wave and sub-millimeter phased arrays and THz Schottky heterodyne receivers for planetary science and heliophysics.



**P. Hartogh, Dr.** Paul Hartogh received the M.Sc. and Ph.D. degrees in physics from the University of Göttingen, Göttingen, Germany, in 1985 and 1989, respectively. He has been a Staff Member with the Max Planck Institute for Solar System Research, Göttingen, since 1990. He developed microwave and far infrared instrumentation for observations of the earth and extraterrestrial atmospheres. He was the Principal Investigator of the Herschel solar system observation program on “Water and Related Chemistry in the Solar System” and is currently the PI of the Submillimetre Wave Instrument (SWI) on the Jupiter ICy moons Explorer (JUICE). He was a Co-Investigator (Co-I) of the Millimeter Wave Atmospheric Sounder (MAS) on Space Shuttle (Atlas 1–3) and is currently the Co-I of the Microwave Instrument for the Rosetta Orbiter (MIRO), the German REceiver for Astronomy at THz frequencies (GREAT) on the Stratospheric Observatory For Infrared Astronomy (SOFIA) and he is Co-PI of ESA's M4 mission Atmospheric Remote-sensing Infrared Exoplanet Large-survey (ARIEL). He is a member of the Science Definition Team of ESA's M4 mission Atmospheric Remote-Sensing Exoplanet Large-Survey.